International Journal of Engineering

Journal Homepage: www.ije.ir

Seismic Vulnerability of Irregular Reinforced Concrete Buildings Considering the Soil-structure Interaction

S. El Janous*, A. El Ghoulbzouri

Laboratory of Applied Sciences, National School of Applied Sciences AL Hoceima, University AbdelmalekEssaadi, Tetouan, Morocco

PAPER INFO

Paper history:
Received 21 July 2023
Received in revised form 16 Augut 2023
Accepted 20 August 2023

Keywords:
Plastic Hinges
Seismic Response
Fragility Curves

ABSTRACT

In this study, we present an investigation into the seismic vulnerability assessment of medium-rise reinforced concrete structures featuring vertical geometric irregularity (setback). We considered the effects of the percentage and location of the setback along the height of the building, as well as the impact of changing site classes. Additionally, we incorporated the effects of soil-structure interaction into the nonlinear response of the building. In the first part, we investigated the influence of the aforementioned parameters on the seismic response of a structure through nonlinear static analyses. We analyzed the capacity curves and the development of plastic hinges in the structural elements. In the second part, we analyzed the seismic fragility of building frames using a probabilistic study approach. We developed fragility curves to assess the vulnerability of the structures.In conclusion, the obtained results highlight the fundamental importance of considering structural irregularities as well as the impact of different site classes on the seismic vulnerability of buildings.

***doi**: 10.5829/ije.2024.37.01a.10*

NOMENCLATURE

μ_u	The ultimate ductility	$\overline{T}$	Period of the flexible-base structure
G	Shear modulus of the soil	ρ	Density
G_0	Initial shear modulus	D_y	Elastic displacement
L	Length of the foundation	V_y	Elastic shear velocity
B	Width of the foundation	I_f	Moment of inertial
υ	Poisson's ration	A_f	The area of foundation
$\tilde{\varepsilon}$	Total system damping	$r_u = \sqrt{A_f/\pi}$	The foundation radii of translation
ε_f	Damping of the foundation	$r_\theta = \sqrt[4]{4 \times I_F/\pi}$	The foundation radii of rotation
ε_i	Damping of the structure	$K_u = \frac{8}{2-\nu} \times G \times r_u$	The static stiffness of a disk on a half-space for translational deformation modes
T	Period of the fixed-base structure	$K_\theta = \frac{8}{3(1-\nu)} \times G \times r_\theta$	The static stiffness of a disk in a half-space for rotational deformation modes
D_u	The ultimate displacement		

1. INTRODUCTION

Research into vertical irregularities in buildings has been an active field of study since the 1970s. Several researchers have played a pioneering role in this field. Chopra and Kan (1) focused their study on the seismic response of eight-storey buildings, subjecting them to seismic ground motion data.

Similarly, Ruiz and Diederich (2) carried out analytical studies on models of five- and twelve-storey buildings with irregularities in resistance. The impact of building setback on the seismic response of multi-storey structures was assessed by Shahrooz and Moehle (3).

Valmundsson and Nau (4) undertook a parametric

*CorrespondingAuthorEmail: *soumaya.eljanous@etu.uae.ac.ma*
(S. El Janous)

Please cite this article as: El Janous S, El Ghoulbzouri A. Seismic Vulnerability of Irregular Reinforced Concrete Buildings Considering the Soil-structure Interaction. International Journal of Engineering, Transactions A: Basics. 2024;37(01):104-114.

study of two-dimensional building structures with irregularities in mass, stiffness and strength. Their results indicate that strength irregularities have the most significant influence on response compared to mass and stiffness irregularities.

In another relevant study, Michalis et al. (5) examined the effect of vertical irregularities on the capacity of a 9-storey building using incremental dynamic analysis (IDA). They concluded that irregularities have a substantial impact on boundary states and depend on earthquake intensity.

As for Shaikh and Shinde (6), their interest focused on the seismic response of a reinforced concrete frame presenting a vertical irregularity associated with a mass irregularity.

Furthermore, Shah et al. (7) carried out a study on the seismic risk assessment of mid-rise steel buildings, highlighting different types of vertical irregularities, such as mass, stiffness and/or resistance irregularities.

In a recent study, Kyoung et al. (8) proposed a simplified modeling method to examine the behavior of buildings with irregularities. Their approach consists of transforming vertically irregular structures into geometrically regular ones using a floor stiffness equation.

Also Hait et al. (9) confirmed that the buildings with irregular configurations suffer greater damage than those with regular contours, mainly due to the increased influence of torsional effects.

On the other hand, Mouhine and Hilali (10) assessed the seismic vulnerability of twenty building structures with vertical geometric irregularities at different positions. They adopted a probabilistic approach based on non-linear static analysis to calculate damage probabilities. The results revealed that the percentage of shrinkage has a significant impact on the dynamic response of irregular structures and modifies building performance.

As part of our research, we focused on studying the seismic behavior of reinforced concrete buildings with vertical geometric irregularities, taking into account soil-structure interaction. We carried out three-dimensional simulations of medium-sized building structures, including shrinkage, using SAP 2000 finite element analysis software.

2. SOIL-STRUCTURE INTERACTION

2. 1. Non-linear Approach for Assessing the Seismic Performance of Strutures We introduce a simplified model tailored to address the intricate challenges posed by nonlinear soil-structure interaction (SSI). The N2 method, originally formulated by Fajfar (11), is employed to assess the nonlinear behavior of the structure. In its initial version, this method assumes a fixed structure base, thereby excluding the influence of soil-structure interaction (SSI). Our proposed approach, named the N2-SSI method, extends the N2 method to incorporate soil effects into the nonlinear response (12).

2. 2. Foundation Impedances The deformations of the structure during seismic shaking are affected by the interactions among the three interconnected systems: the structure, the foundation, and the geological media underlying and surrounding the foundations.

When a structure is built on soft soil, it is generally more susceptible to significant deformations compared to if it were erected on rock soil. As a result, various issues can arise, such as cracking due to differential settlements (13, 14).

The consideration of soil-structure interaction is accomplished by integrating a system of springs and dampers. The foundation and its interaction with the soil (spring-dampers) are modeled using impedance functions. The expression for these foundation impedances is cited in Table 1 according to the FEMA 356 (15) standard.

2. 3. Damping and the Effective Period of the Soil-structure System Typically, a damping coefficient of 5% is employed in dynamic analyses for ordinary structures experiencing seismic forces. Nevertheless, this value holds limited significance for reinforced concrete buildings when considering Soil-Structure Interaction (SSI). Soil exhibits two forms of damping: internal damping caused by the soil's hysteresis (hysteretic damping), and damping resulting from the dispersion of seismic waves (radial damping).

To account for the increase in damping, Veletsos and Nair (16) propose the following similar Equation 1:

$$\tilde{\varepsilon} = \varepsilon_f + \frac{\varepsilon_i}{(\frac{\bar{T}^3}{T^3})} \quad (1)$$

In the given equation, the total system damping is calculated by adding the damping of the foundation to a

TABLE 1. Foundation impedances and total damping for the cases studied

Degrees of Freedom	Foundation impedances
Translation along the x-axis	$K_x = \frac{GB}{2-\upsilon}[3.4\left(\frac{L}{B}\right)^{0.65} + 1.2]$
Translation along the y-axis	$K_y = \frac{GB}{2-\upsilon}[3.4\left(\frac{L}{B}\right)^{0.65} + 0.4\frac{L}{B} + 0.8]$
Translation along the z-axis	$K_z = \frac{GB}{1-\upsilon}[1.55\left(\frac{L}{B}\right)^{0.75} + 0.8]$
Rotation about the x-axis	$K_{xx} = \frac{GB^3}{1-\upsilon}[0.4\frac{L}{B} + 0.1]$
Rotation about the y-axis	$K_{yy} = \frac{GB^3}{1-\upsilon}[0.47\left(\frac{L}{B}\right)^{2.4} + 0.034]$
Rotation about the z-axis	$K_{zz} = GB^3[0.53\left(\frac{L}{B}\right)^{2.45} + 0.51]$

portion of the structure's damping, which is typically assumed to be 5% for conventional structures.

When determining the effective period, we can combine the two expressions for the period, using both the fixed T (rigid foundation) and $\overline{T}$ (flexible foundation) as bases (17), and it is easy to arrive at Equation 2:

$$\frac{\overline{T}}{T} = \sqrt{1 + \frac{K}{K_u} + \frac{Kh_{eff}^{\ 2}}{K_\theta}} \quad (2)$$

2. 4. The Results of Foundation Impedances and Total Damping for the Soil-structure System Used

Table 2 displays the values of spring stiffness corresponding to different directions, based on the shear wave velocity of the soil for each given site category. These values are specific to a foundation with a section of 18.47x3 m².

3. DEVELOPMENT OF FRAGILITY CURVES

Conducting a quantitative assessment of the likelihood of seismic damage under various seismic loads is crucial. In this context, seismic fragility analysis serves as a significant approach for evaluating the chances of structures or components surpassing a predefined damage threshold when exposed to progressively stronger seismic ground motions (18-22).

This method has been utilized to evaluate the susceptibility of diverse structures to seismic events.

Fragility curves represent the relationship between a specific seismic intensity parameter, such as peak acceleration, spectral intensity, or macroseismic intensity, and the estimated average damage value of a structure. These curves are utilized to evaluate the vulnerability of a particular building and estimate the potential damage it may experience in the event of an earthquake.

The fragility curve follows a logarithmic function in a normal distribution and can be described by the following Equation 4:

$$P(dsi/S_d) = \phi\left(\frac{1}{\beta_{dsi}} \times \ln\left(\frac{S_d}{\overline{S_{d,dsı}}}\right)\right) \quad (4)$$

where, β_{dsi} is the standard deviation of the logarithm of the spectral displacement of the damage state dsiand ϕ is the normal distribution function.

Threshold values $\overline{S_{d,dsı}}$ are given as a function of Dy and the ultimate displacement Du of the structure. For β_{dsi} is calculated directly as a function of μ_u (see Table 3):

4. THE GEOMETRIC CHARACTERISTICS OF THE STRUCTURES STUDIED

The following section focuses on quantifying the vulnerability of six reinforced concrete irregular

TABLE 2. The foundation impedances and total damping for the studied cases.

Total damping		Degrees of freedom	Foundation impedances (* 10^9 N/m)
Soil A	5%	translation along the x-axis 10^9 N/m	18445.92927
		translation along the y-axis 10^9 N/m	26978.8793
		translation along the z-axis 10^9 N/m	21565.30743
		rotation about the x-axis 10^9 N.m/rd	76129.92582
		rotation about the y-axis 10^9 N.m/rd	980618.9313
		rotation about the z-axis 10^9 N.m/rd	852367.2701
Soil B	5%	translation along the x-axis 10^9 N/m	88,86664316
		translation along the y-axis 10^9 N/m	129,975693
		translation along the z-axis 10^9 N/m	103,8948189
Soil B	5%	rotation about the x-axis 10^9 N.m/rd	366,769863
		rotation about the y-axis 10^9 N.m/rd	4724,31133
		rotation about the z-axis 10^9 N.m/rd	4106,435459
		translation along the x-axis 10^9 N/m	12,9697263
		translation along the y-axis 10^9 N/m	18,96942546
		translation along the z-axis 10^9 N/m	15,16302762
Soil C	6%	rotation about the x-axis 10^9 N.m/rd	53,5285746
		rotation about the y-axis 10^9 N.m/rd	689,4940859
		rotation about the z-axis 10^9 N.m/rd	599,3176075
		translation along the x-axis 10^9 N/m	1,045263868
		translation along the y-axis 10^9 N/m	1,528795178
		translation along the z-axis 10^9 N/m	1,222027707
Soil D	13%	rotation about the x-axis 10^9 N.m/rd	4,314006605
		rotation about the y-axis 10^9 N.m/rd	55,56811596
		rotation about the z-axis 10^9 N.m/rd	48,30055978

TABLE 3. Damage threshold values

Damage status thresholds	Definition	β_{dsi}	The state of damage
$\overline{Sd}_{ds1}$	0.7 D_y	$\beta_{ds1} = 0.25 + 0.07 \ln(\mu_u)$	Light
$\overline{Sd}_{ds2}$	D_y	$\beta_{ds2} = 0.2 + 0.18 \ln(\mu_u)$	Moderate
$\overline{Sd}_{ds3}$	$D_y + 0.25 (D_u - D_y)$	$\beta_{ds3} = 0.1 + 0.4 \ln(\mu_u)$	Severe
$\overline{Sd}_{ds4}$	D_u	$\beta_{ds4} = 0.15 + 0.5 \ln(\mu_u)$	Complete

buildings, in accordance with FEMA 440 (23) standards. The column dimensions are 30x30 cm², and the beam dimensions are 25x30 cm², with a floor height of 3 meters, as shown in Table 4. The buildings are also depicted in Figure 1.

The structure is subjected to a live load of 2 kN/m^2 and a dead load of 7 kN/m^2.

Table 5 presents the properties of four different types of soil on which the studied structures are founded. The SAP2000 software was used to conduct numerical studies.

5. RESULTS AND DISCUSSION

5. 1. Capacity Curves and Plastic Hinge Development Using nonlinear static analyses (24, 25), capacity curves have been constructed for structures S1-1, S1-2, and S1-3, as well as S2-1, S2-2, and S2-3, for each soil type, as illustrated in Figures 2-9. Subsequently, the development of plastic hinges in the structural elements of the six reinforced concrete buildings with irregularities has been examined.

TABLE 4. Details of the structural elements

Type of structure	Type of section	Reinforcement	
Column	(30x30) cm^2	12T12	
Beam	(25x30) cm^2	Top	Upper
		3T10	6T10

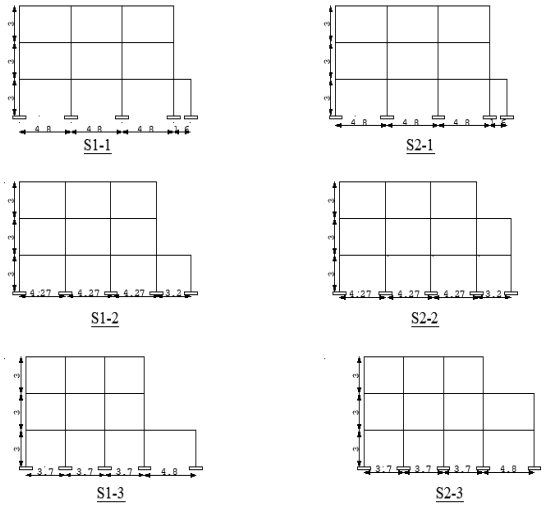

Figure 1. X-Z plan view of the studied construction models with vertical geometric irregularity

TABLE 5. The characteristics of the soils

Soil type	Description	G_0 (N/m) *10^6
Soil A	Rock soil	689475,6
Soil B	Hard soil	3321,675
Soil C	Soft soil	484,785
Soil D	Very soft soil	39,07008

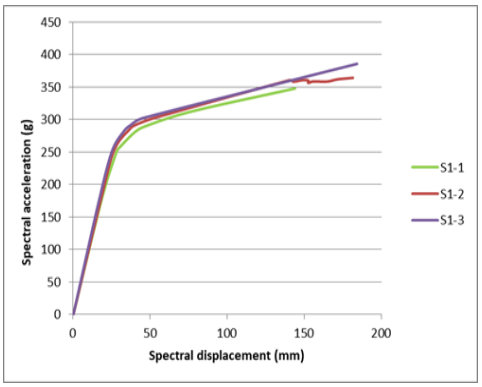

Figure 2. The capacity curves for the studied building models for soil type A (S1-1;S1-2;S1-3)

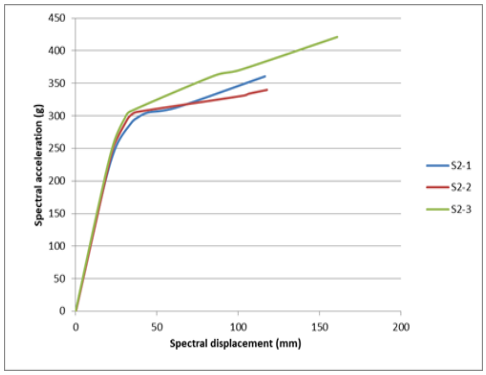

Figure 3. The capacity curves for the studied building models for soil type A (S2-1;S2-2;S2-3)

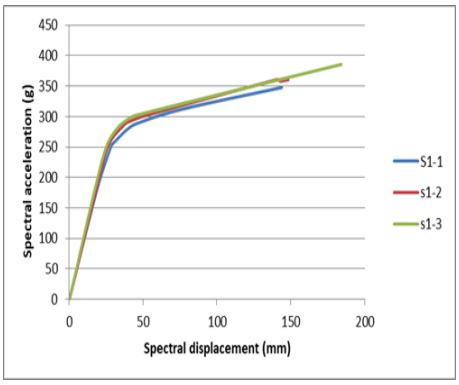

Figure 4. The capacity curves for the studied building models for soil type B (S1-1;S1-2;S1-3)

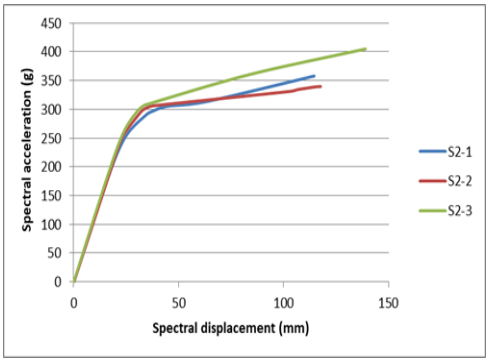

Figure 5. The capacity curves for the studied building models for soil type B (S2-1;S2-2;S2-3)

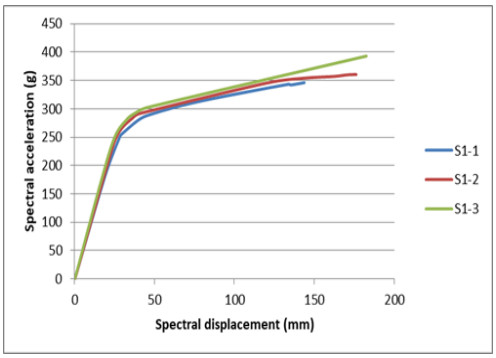

Figure 6. The capacity curves for the studied building models for soil type C (S1-1;S1-2;S1-3)

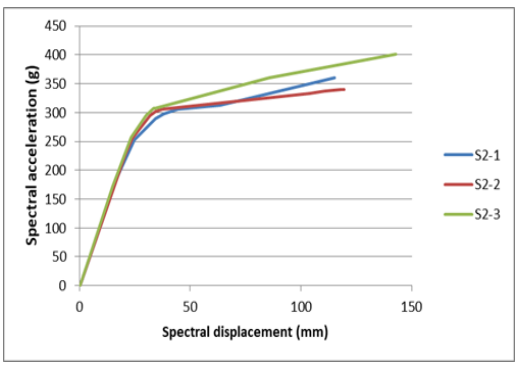

Figure 7. The capacity curves for the studied building models for soil type C (S2-1;S2-2;S2-3)

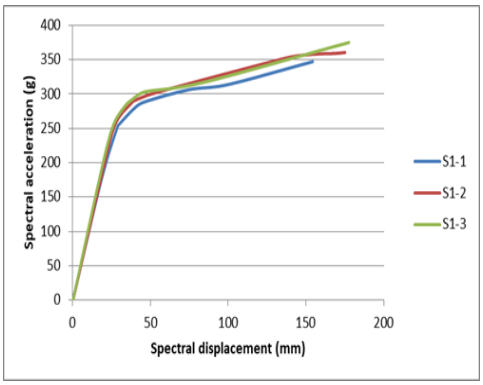

Figure 8. The capacity curves for the studied building models for soil type D (S1-1;S1-2;S1-3)

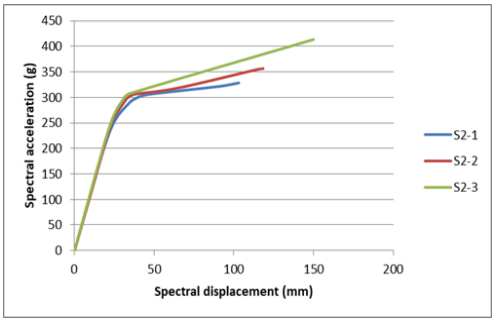

Figure 9. The capacity curves for the studied building models for soil type D (S2-1;S2-2;S2-3)

5. 1. 1. The Capacity Curves Based on the nonlinear static analysis PUSHOVER, capacity curves were established for each building and each soil type, as shown in Figures 2-9. Using these curves, capacity spectra were defined, and elastic capacity points for the modeled reinforced concrete buildings were identified, as indicated in Table 6. The results presented in Table 7 reveal that the setback value and soil type have an influence on the elastic capacity of the building. A significant reduction of 16% is observed for the S1 model with soil types A and B, and a reduction of approximately 11% for the S2 model.

For soil type C, a significant reduction of 16.41% is observed for the S1 model, and a reduction of approximately 11% is observed for the S2 model.

For soil type D, a notable reduction of 14% is observed for the S1 model, and a reduction of approximately 13.5% is observed for the S2 model.

Table 6 reveals that the displacement corresponding to the performance point decreases with an increase in the setback value, particularly for soil types C and D. This indicates that the setback has an influence on the inelastic deformation capacity of the structure during an earthquake, which explains the observed reduction in seismic performance. Consequently, the ductility of the structure will be diminished, potentially leading to significant energy release and damage to the structural elements of the buildings.

TABLE 6. Performance points for the studied buildings

Soil type	Type of structure	Performance point	
		V (kN)	D (mm)
Soil A	S1-1	17.143	1.95
	S1-2	16.486	1.93
	S1-3	15.859	1.696
	S2-1	18.804	1.825
	S2-2	18.512	1.936
	S2-3	18.274	1.676
Soil B	S1-1	21.429	2.397
	S1-2	20.607	2.345
	S1-3	19.823	2.072
	S2-1	23.51	2.249
	S2-2	23.129	2.355
	S2-3	22.828	2.079
Soil C	S1-1	20.293	2.273
	S1-2	19.514	2.236
	S1-3	18.771	1.976
	S2-1	22.262	2.124
	S2-2	21.902	2.243
	S2-3	21.616	1.978
Soil D	S1-1	14.773	1.626
	S1-2	14.201	1.7
	S1-3	13.66	1.527
	S2-1	16.19	1.43
	S2-2	15.936	1.685
	S2-3	15.727	1.512

TABLE 7. Elastic capacity of the studied buildings

Soil type	Type of structure	Elastic capacity	
		Vy (kN)	Dy (mm)
Soil A	S1-1	181.51	19.12
	S1-2	178.76	18.28
	S1-3	166.43	15.97
	S2-1	185.75	16.92
	S2-2	228.89	20.82
	S2-3	173.11	15.11
Soil B	S1-1	181.51	19.1
	S1-2	178.76	18.28
	S1-3	166.43	16
	S2-1	185.77	16.91
	S2-2	228.85	20.86
	S2-3	172.20	15.09
Soil C	S1-1	181.16	19.13
	S1-2	178.80	18.30
	S1-3	166.51	15.99
	S2-1	185.92	16.93
	S2-2	228.91	20.88
	S2-3	171.86	15.08
Soil D	S1-1	178.56	18.89
	S1-2	179.31	18.48
	S1-3	167.37	16.24
	S2-1	187.58	17.25
	S2-2	229.54	21.08
	S2-3	168.07	14.92

5. 1. 2.Distribution of Plastic Hinges The finite element software SAP2000 offers the capability to visualize the development of plastic hinges in structural elements. This allows for tracking and analyzing the behavior of the structure when subjected to loads, particularly in identifying areas where plastic deformations occur and plastic hinges form. This functionality is crucial for evaluating the ductility of the structure and understanding its response to extreme loads, such as those generated by an earthquake. Figures 10-15 provide an illustration of the distribution of plastic hinges for each building on each soil type. They highlight the presence of plastic hinges in most of the columns on the first and second floors, as well as in some columns on the third floor. These images allow for visualizing the areas of plastic deformation and identifying the structural elements that experience the most significant deformations during an earthquake.

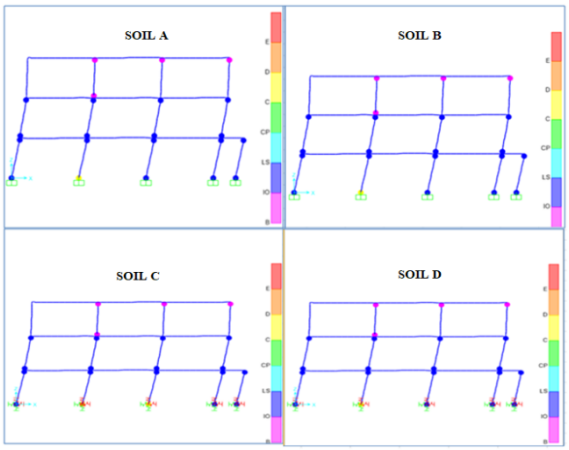

Figure 10. The development of plastic hinges in structural elements for the model S1-1

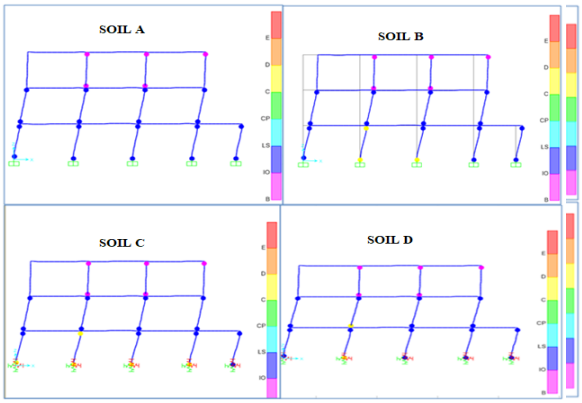

Figure 11. The development of plastic hinges in structural elements for the model S1-2

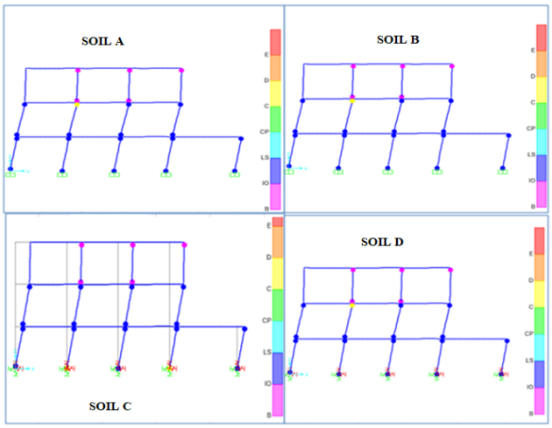

Figure 12. The development of plastic hinges in structural elements for the model S1-3

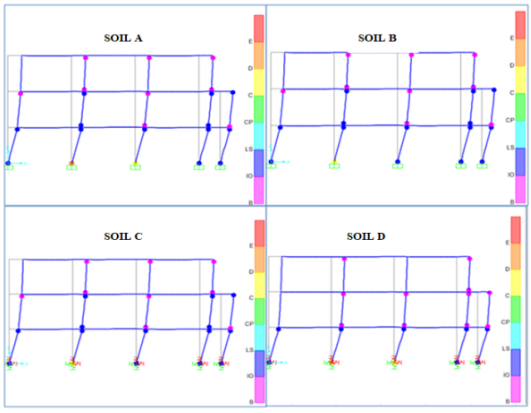

Figure 13. The development of plastic hinges in structural elements for the model S2-1

As the applied force and rotation of the plastic hinges increase, different types of hinges can be observed. For cases S1-1, S1-2, and S1-3 on soil types A and B, Type B, Type Intermediate Opening (IO), and Type C hinges are observed. This suggests the presence of damage in the

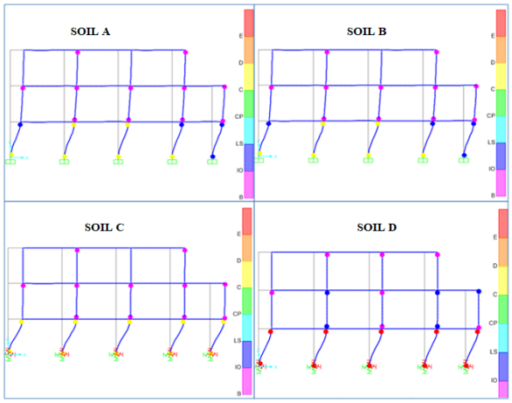

Figure 14. The development of plastic hinges in structural elements for the model S2-1

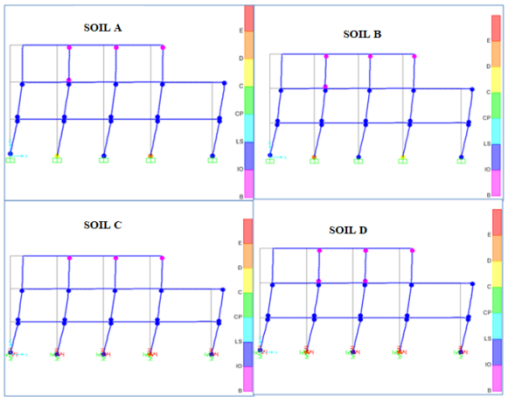

Figure 15. The development of plastic hinges in structural elements for the model S2-3

structure, but it is not yet considered to be very significant.

However, for soil types C and D, the appearance of Type D hinges is observed in addition to the other types mentioned earlier. This observation indicates the presence of more significant damage in the structure, requiring special attention.

These observations help in understanding the evolution of structural behavior and identifying the most vulnerable areas to damage during an earthquake.

By examining cases S2-1, S2-2, and S2-3, it is observed that for soil types A and B, Type B, Type IO, Type C, and Type D, hinges are formed. However, for soil types C and D, the appearance of Type E hinges is also observed, indicating a higher level of damage that could lead to structural failure.

These observations lead us to conclude that vertical geometric irregularities at different levels, as well as the soil type, have a negative influence on the behavior of the structure during an earthquake. Vertical geometric irregularities can result in stress concentration and an uneven redistribution of seismic forces, leading to zones that are more vulnerable to damage. Additionally, soil

characteristics such as stiffness and the ability to dissipate seismic energy can also play a significant role in the overall behavior of the structure.

5. 2.Curves of Fragility The fragility curves are created through the compilation of seismic intensity values associated with a particular soil type until they align with a pre-established damage intensity threshold. These curves adeptly illustrate the propagation of seismic intensity influenced by variations in soil characteristics, highlighting a substantial likelihood of reaching or surpassing a notable level of seismic damage (26-28).

The vulnerability of a typical reinforced concrete structure will be analyzed using a seismic performance approach that integrates the effects of Soil-Structure Interaction (SSI) into the nonlinear response .

Fragility curves are constructed to assess the probability of exceeding different seismic intensities, as illustrated in Figures 16-19. The probability of exceeding is determined using Equation 4. The damages probabilities are shown in Figure 20; these are computed taking into account the performance points of each structure.

This approach allows for estimating the probability of experiencing different levels of damage based on the seismic intensity. It provides valuable insights to assess the vulnerability of the structure and make informed decisions regarding design and seismic strengthening.

Figure 20 displays the calculated damage probabilities for various construction models based on different site classes. The results emphasize the critical

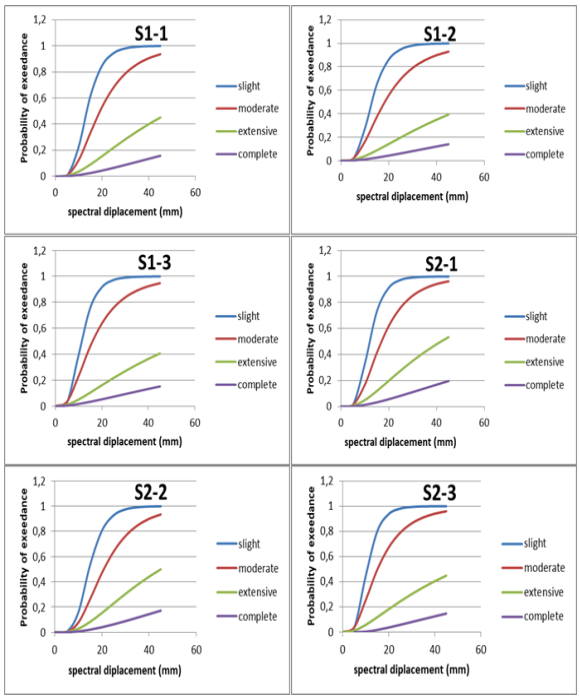

Figure 16. Fragility curves for Soil A

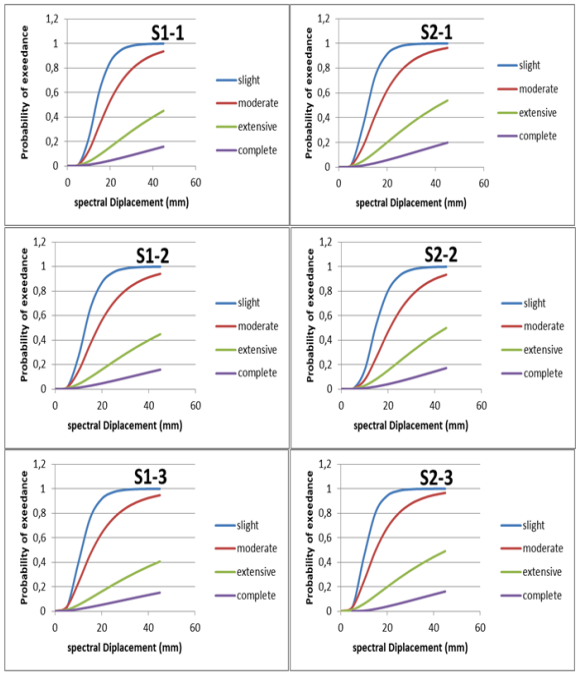

Figure 17. Fragility curves for Soil B

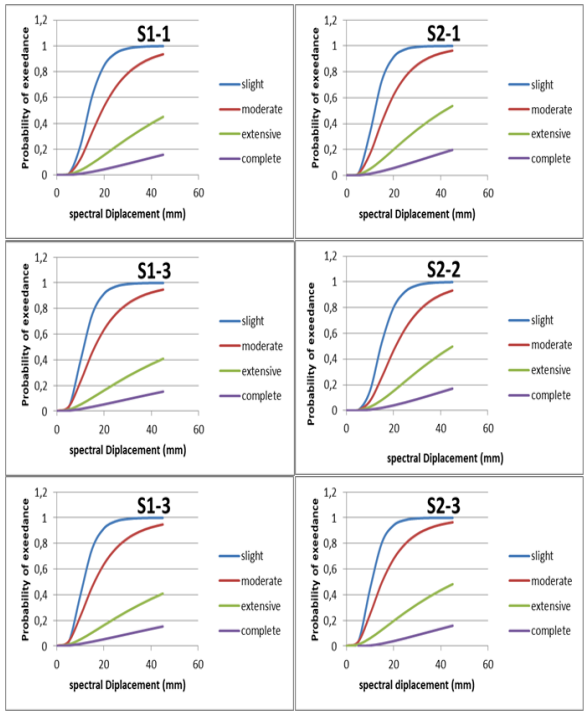

Figure 18. Fragility curves for Soil C

significance of site selection in seismic vulnerability analysis.

Structures constructed on soil types A and B exhibit low damage probabilities, regardless of the damage state under consideration. Conversely, structures built on soil

types C and D demonstrate higher damage probabilities. This trend remains consistent regardless of the setback position along the building height.

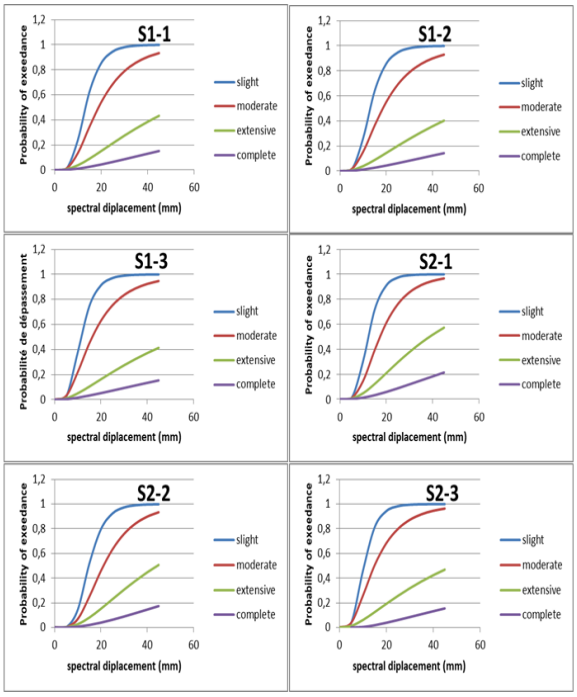

Figure 19. Fragility curves for Soil D

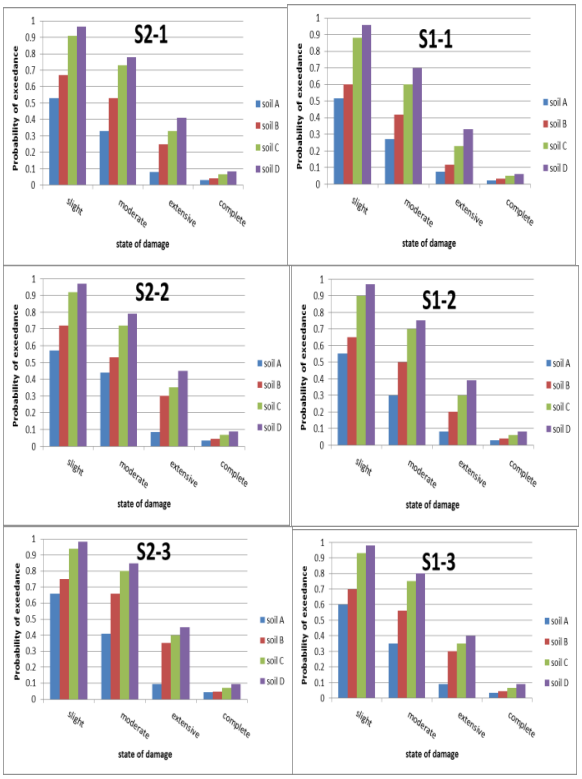

Figure 20. The effect of soil type on the seismic vulnerability of the studied models

It has been confirmed that the behavior of a structure is influenced not just by its motion characteristics and the specifics of the seismic forces it experiences, but also by the surrounding external conditions at its foundation. This encompasses the interplay between the structure, its base, and the underlying soil (29-31).

Furthermore, Figure 20 illustrates the considerable influence of shrinkage position on the probability of damage. As the building height increases, so does the likelihood of damage. In other words, the probability of damage rises as the shrinkage exceeds one storey.

These observations underscore the importance of considering both site selection and setback position when analyzing the seismic vulnerability of building structures (32). This comprehensive analysis provides a better understanding of the risks associated with different seismic scenarios and guides decisions on seismic design and strengthening. Incorporating these considerations is essential for enhancing the resilience of buildings against potential earthquakes.

6. CONCLUSIONS

The objective of this research was to investigate the impact of changing site class and incorporating Soil-Structure Interaction (SSI) effects on the structural vulnerability of irregular reinforced concrete buildings during earthquakes.

The main conclusions drawn from this study are as follows:

- Ultimate Capacity and Plastic Hinge Development:

The results of the study highlighted the influence of vertical geometric irregularity and changing soil class on the behavior of the structure. In the case of soft soil conditions, a significant decrease in the building's elastic capacity is evident. The S1 model displays a reduction of about 14%, while the S2 model shows an approximate reduction of 13.50%.

The development of plastic hinges in structural elements and the ultimate capacity of the building were notably affected. As the setback margin value increased, the structural fragility of reinforced concrete buildings also increased. Therefore, it can be concluded that the degree of vertical geometric irregularity has a significant impact on the performance of building structures. Higher irregularity values lead to a more pronounced reduction in inelastic deformation capacity.

- Damage Probabilities and Site Selection:

The calculated damage probabilities for different building models underscore the importance of site selection in seismic vulnerability analysis. Structures constructed on rocky soil exhibit low probabilities of damage, regardless of the considered damage state. In contrast, buildings erected on loose soil show higher probabilities of damage.

- Significance of Site Class and Geometric Irregularity:

The research highlights that both site class and geometric irregularity are crucial factors influencing the seismic vulnerability of these structures. During the structural analysis phase, it is vital to take these aspects into account to better understand the associated risks and implement appropriate design and reinforcement measures.

Considering these findings, it becomes evident that a comprehensive seismic risk assessment should consider both site selection and geometric irregularity to ensure the safety and resilience of irregular reinforced concrete buildings during earthquakes. Properly accounting for these factors in the design and strengthening processes will lead to more effective mitigation strategies and safer structures.

7. REFERENCES

1. Chopra AK, Kan C. Effects of stiffness degradation on ductility requirements for multistorey buildings. Earthquake Engineering & Structural Dynamics. 1973;2(1):35-45. 10.1002/eqe.4290020104
2. Ruiz S, Diederich R. The Mexico earthquake of September 19, 1985—the seismic performance of buildings with weak first storey. Earthquake Spectra. 1989;5(1):89-102. 10.1193/1.1585512
3. Shahrooz BM, Moehle JP. Seismic response and design of setback buildings. Journal of Structural Engineering. 1990;116(5):1423-39. 10.1061/(ASCE)0733-9445(1990)116:5(1423)
4. Valmundsson EV, Nau JM. Seismic response of building frames with vertical structural irregularities. Journal of Structural Engineering. 1997;123(1):30-41. 10.1061/(ASCE)0733-9445(1997)123:1(30)
5. Michalis F, Dimitrios V, Manolis P. Evaluation of the Influence of Vertical Irregularities on the Seismic Performance of a 9-storey steel frame. 10.1002/eqe.591
6. Sameer JS, Shinde S. Seismic response of vertically irregular RC frame with mass irregularity. International Journal of Civil Engineering and Technology. 2016;7(5):2016. IJCIET_07_05_028
7. Shah BM, Davis R, Nandakumar C, Sarkar P, editors. Review of Performance of Existing Vertical Irregularity Indicators for Steel Framed Buildings. Proceedings of SECON 2020: Structural Engineering and Construction Management 4; 2021: Springer.
8. Ro KM, Kim MS, Lee YH. A simplified approach to modeling vertically irregular structures for dynamic assessment. Journal of Asian Architecture and Building Engineering. 2022;21(6):2320-9. 10.1080/13467581.2021.1971682
9. Hait P, Sil A, Choudhury S. Damage assessment of reinforced concrete buildings considering irregularities (research note). International Journal of Engineering. 2019;32(10):1388-94. 10.5829/ije.2019.32.10a.08
10. Mouhine M, Hilali E. Seismic vulnerability assessment of RC buildings with setback irregularity. Ain Shams Engineering Journal. 2022;13(1):101486. 10.1016/j.asej.2021.05.001
11. Miranda E, Bertero VV. Evaluation of strength reduction factors for earthquake-resistant design. Earthquake Spectra. 1994;10(2):357-79.
12. Mekki M, Elachachi S, Breysse D, Zoutat M. Seismic behavior of RC structures including soil-structure interaction and soil variability effects. Engineering Structures. 2016;126:15-26. 10.1016/j.engstruct.2016.07.03428
13. Zhang X, Far H. Seismic Response of High-Rise Frame–Shear Wall Buildings under the Influence of Dynamic Soil–Structure Interaction. International Journal of Geomechanics. 2023;23(9):04023141. 10.1061/IJGNAI.GMENG-845
14. Aydin E, Ozturk B, Bogdanovic A, Farsangi EN, editors. Influence of soil-structure interaction (SSI) on optimal design of passive damping devices. Structures; 2020: Elsevier. 10.1016/j.istruc.2020.09.028
15. Safety IS. Recommended Provisions for Seismic Regulations for New Buildings and Other Structures (FEMA 450). FEMA: Washington, DC, USA. 2003.
16. Veletsos AS, Nair VD. Seismic interaction of structures on hysteretic foundations. Journal of the Structural Division. 1975;101(1):109-29. 10.1016/j.asej.2021.05.001
17. Veletsos AS, Verbič B. Vibration of viscoelastic foundations. Earthquake Engineering & Structural Dynamics. 1973;2(1):87-102. 10.1002/eqe.4290020108
18. Pan H, Li C, Tian L. Seismic fragility analysis of transmission towers considering effects of soil-structure interaction and depth-varying ground motion inputs. Bulletin of Earthquake Engineering. 2021;19(11):4311-37. 10.1007/s10518-021-01124-x
19. Kassem MM, Nazri FM, Farsangi EN, Ozturk B. Improved vulnerability index methodology to quantify seismic risk and loss assessment in reinforced concrete buildings. Journal of Earthquake Engineering. 2022;26(12):6172-207. 10.1080/13632469.2021.1911888
20. Kassem MM, Nazri FM, Farsangi EN, Ozturk B. Development of a uniform seismic vulnerability index framework for reinforced concrete building typology. Journal of Building Engineering. 2022;47:103838. https://doi.org/10.1016/j.jobe.2021.103838
21. Ozturk B, Sahin HE, Yildiz C, editors. Seismic performance assessment of industrial structures in turkey using the fragility curves. 15th World Conference on Earthquake Engineering, Lisbon, Portugal; 2012.
22. Nair S, Hemalatha G, Stephen E. Seismic vulnerability studies of a g+ 17 storey building in abu dhabi-uae using fragility curves. International Journal of Engineering, Transactions B: Applications. 2021;34(5):1167-75. 10.5829/IJE.2021.34.05B.10
23. Council AT. Improvement of nonlinear static seismic analysis procedures: FEMA Region II; 2005.
24. Chopra AK, Goel RK. A modal pushover analysis procedure for estimating seismic demands for buildings. Earthquake engineering & structural dynamics. 2002;31(3):561-82. 10.1002/eqe.144
25. Chintanapakdee C, Chopra AK. Evaluation of modal pushover analysis using generic frames. Earthquake engineering & structural dynamics. 2003;32(3):417-42. 10.1002/eqe.232
26. Porter K, Kennedy R, Bachman R. Creating fragility functions for performance-based earthquake engineering. Earthquake spectra. 2007;23(2):471-89. 10.1193/1.2720892
27. Park Y-J, Ang AH-S, Wen YK. Seismic damage analysis of reinforced concrete buildings. Journal of Structural Engineering. 1985;111(4):740-57. 10.1061/(ASCE)0733-9445(1985)111:4(740)
28. Taliakula P, Prasad DV. Seismic fragility analysis of regular and vertical setback R/C frame buildings. Int Journal of Engineering Research and Applications, ISSN. 2015:2248-9622.
29. Mekki M, Elachachi S, Breysse D, Nedjar D, Zoutat M. Soil-structure interaction effects on RC structures within a performance-based earthquake engineering framework. European

Journal of Environmental and Civil Engineering. 2014;18(8):945-62. 10.1080/19648189.2014.917056

30. Sharanya A, Heeralal M, Thyagaraj T. Soil shrinkage characterization of low plasticity soil using digital image analysis process. International Journal of Engineering, Transactions A: Basics. 2021;34(10):2206-12. 10.5829/ije.2021.34.10a.02
31. Shirzadi M, Behnamfar F, Asadi P. Effects of soil–structure interaction on inelastic response of torsionally-coupled structures. Bulletin of Earthquake Engineering. 2020;18:1213-43. 10.1007/s10518-019-00747-5
32. Mouhine M, Hilali E. Seismic vulnerability for irregular reinforced concrete buildings with consideration of site effects. Materials Today: Proceedings. 2022;58:1039-43. 10.1016/j.matpr.2022.01.038

Persian Abstract

چکیده

در این مطالعه، ما تحقیقی در مورد ارزیابی آسیب‌پذیری لرزه‌ای سازه‌های بتن مسلح با ارتفاع متوسط با بی‌نظمی هندسی عمودی (پسرفت) ارائه می‌کنیم. ما تأثیرات درصد و مکان عقب‌نشینی در طول ارتفاع ساختمان و همچنین تأثیر تغییر کلاس‌های سایت را در نظر گرفتیم. علاوه بر این، ما اثرات برهمکنش خاک–ساختار را در پاسخ غیرخطی ساختمان گنجانده ایم. در بخش اول، تأثیر پارامترهای فوق بر پاسخ لرزه‌ای یک سازه را از طریق تحلیل‌های استاتیکی غیرخطی بررسی کردیم. ما منحنی های ظرفیت و توسعه لولاهای پلاستیکی را در عناصر ساختاری تجزیه و تحلیل کردیم. در بخش دوم، شکنندگی لرزه‌ای قاب‌های ساختمان را با استفاده از رویکرد مطالعه احتمالی تحلیل کردیم. ما منحنی‌های شکنندگی را برای ارزیابی آسیب‌پذیری سازه‌ها ایجاد کردیم. در نتیجه، نتایج به‌دست‌آمده اهمیت اساسی در نظر گرفتن بی‌نظمی‌های سازه‌ای و همچنین تأثیر طبقات مختلف سایت بر آسیب‌پذیری لرزه‌ای ساختمان‌ها را برجسته می‌کند.